

Modeling and Analysis of a Rocket Based Combined Cycle Rocket Nozzle

A Kalyan Charan, D Madhava Reddy, CH Rakesh
(Mechanical Department, KNR CER/JNTUH, INDIA)

Abstract : This project develops a rocket nozzle. The nozzle is designed in such a way that the divergent portion of the nozzle geometry must pass through a clover that is placed on the perimeter, thus creating a space for air intake into the centre of an annular rocket exhaust stream. The main objective of this project is to determine the best one from (3clover, 4clover and 5 clovers) and comparison of numerical simulation to a predefined Mach number distribution of in viscid solution and viscous simulation using the $k-\varepsilon$ turbulence model will be attempted. Geometry designs and Meshing were made in ICEM CFD 13.0 and an analysis is carried out in FLUENT 13.0. Based on the flow analysis it is found that nozzle with 4 clovers/gates provides better results when compared with the other i.e., 3 or 5 clovers/gates and it is one of the suggested and effective design of the nozzle. In viscid area-averaged computational results are within 2.1% of the predefined outlet Mach number of 2.75 and 7.6% of the isentropic pressure predicted at the outlet. Viscous computational results obtained using the $k-\varepsilon$ turbulence model under-predict the predefined outlet Mach number by 4% which is acceptable.

Keywords: CFD, Mach, RBCC, Rocket Nozzle.

I. Introduction:

Since propellants can account for upwards of 90% of the vehicle's initial mass^[1, 3] and the high costs required for launch, extensive efforts have gone into the improvement of rocket systems. Major work since the inception of rockets has gone into several fields: (1) Propellant choice; (2) Feed system design; (3) Increasing thrust chamber performance; (4) Maximizing area expansion ratio through improved nozzle design; and (5) Multistaging. Concepts still in development include (6) rocket-based combined cycles and (7) liquid-air cycle engines. The motivation behind these seven concepts is to increase the performance qualifiers thrust FT or specific impulse ISP or reduce initial rocket mass. Five of the seven fields for improving rocket design propellant choice, feed system design, thrust chamber performance, nozzle improvements, and multistaging have been well examined and implemented to the extent that there is very little room for additional improvement. The focus of this research is based on the expectation that entraining air into the centre of an annular rocket exhaust stream causes the ejector effect necessary for the ejector mode of RBCC operation. Anticipated benefits to pursuing this concept include higher thrust due to increased mixing ability between the higher annular rocket exhaust velocity and entrained air along the central axis as compared to entraining air on the annulus with the rocket located along the central axis and a more convenient mounting configuration for an axisymmetric ejector duct since it can be attached directly to the outer wall of the rocket nozzle.

II. Proposed Rocket Nozzle Rbcc:

This project is based on the expectation that entraining air into the centre of an annular rocket exhaust stream as shown in Fig. causes the ejector effect necessary for the ejector mode of RBCC operation.

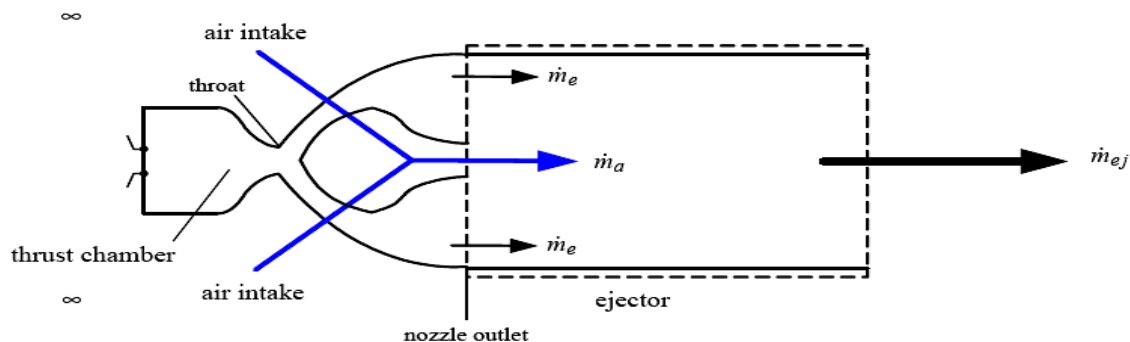


Fig.1 Proposed Rocket Nozzle RBCC.

III. Different Types For Proposed Rocket Nozzle For Rbcc To Increase The Thrust :

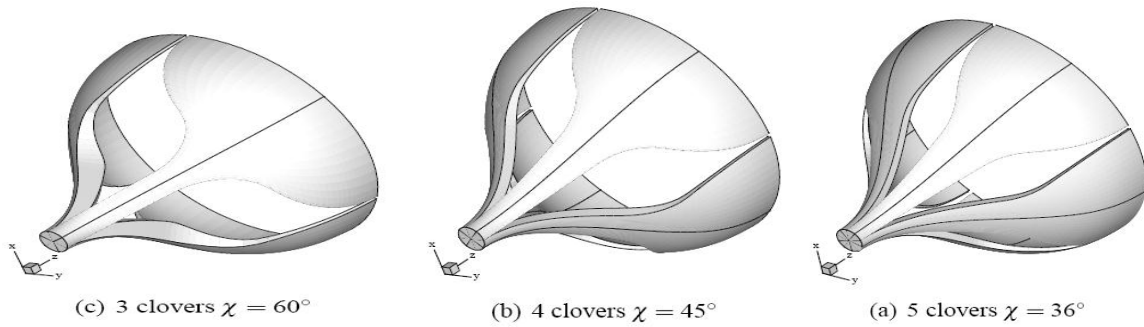


Fig.2 Different Types for Proposed Rocket Nozzle for RBCC.

IV. Design Selection:

The design to be considered in the computational fluid dynamics analyses is developed from the Mach number distribution shown in Fig.3 This $M(z)$ distribution reaches $Me = 2.75$ at the outlet and is created using the theory described in Etele to an Atlas E/F LR-105-5 sustainer engine^[11]. The exhaust flow properties correspond to the products from a kerosene $C_{12}H_{24}$ and air reaction with 100% combustion efficiency and an equivalence ratio of 1.49.

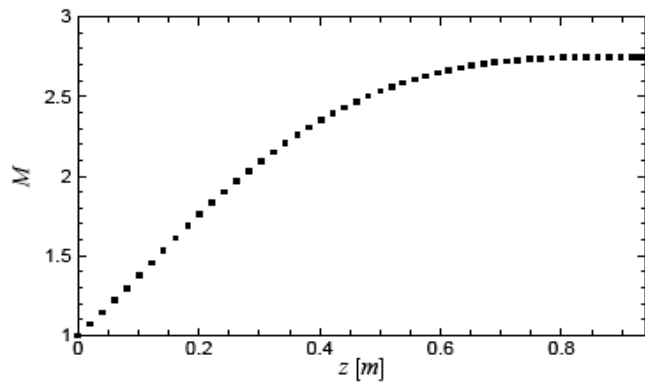
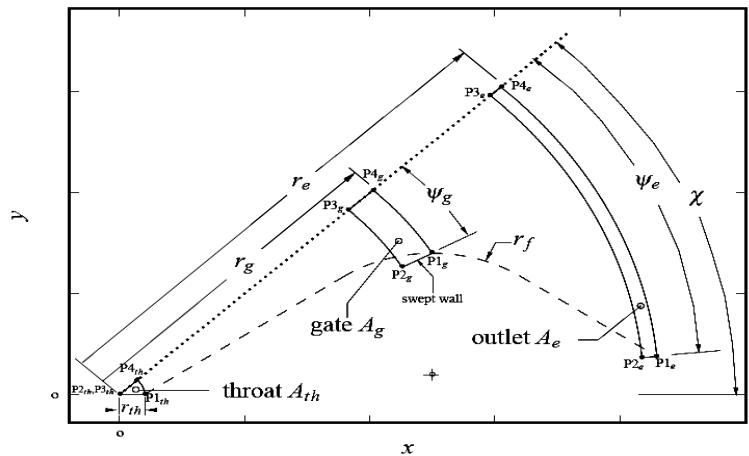


Fig.3 Mach number distribution along nozzle length



V. Geometry Cross Section:

Fig.4 Geometry Cross Section.

Table 1. Geometry reference values for the sensitivity analysis.

Input Variable	Value	Input Variable	Value
χ	45 ⁰	$\frac{z_g}{r_{th}}$	9.5
$\frac{r_g}{r_{th}}$	6.5	ϕ_e	2 ⁰
ψ_g	20 ⁰	$\frac{r_e}{r_{th}}$	10 ⁰
$\frac{r_f}{r_{th}}$	2.5	ψ_e	44 ⁰

Table2. Input geometry variables for selected design.

Variable	Value	Variable	Value
r_{th} [m]	0.0551	z_e [m]	0.9
r_f [m]	0.17	z_g [m]	0.5
r_g [m]	0.37	r_e [m]	0.5
ψ_g	17.6°	ψ_e	44.5°
ϕ_e	1°		

VI. Computational Implementation

- A. The Geometry designs and Meshing were made in ICEM CFD 13.0.
- B. Analyses is carried out in FLUENT 13.0

VII. Fluid Properties

The reference values for enthalpy h_{ref} and entropy s_{ref} are with respect to a pressure of 1[atm] and temperature of 298 [K] and are non-zero because the Fluid mixture considers the products of a $C_{12}H_{24}$ /air reaction. Products by molar fractions consist of 13% carbon dioxide, 13% water vapour, 73.4% nitrogen, and 0.6% of unburned $C_{12}H_{24}$ hydrocarbon.

VIII. Boundary Conditions

For the computations presented throughout this thesis, the throat surface is specified as an inlet boundary condition. A uniform flow with $V = 1114\text{m/s}$ acting normal to the throat cross section is used. This value equates to $M = 1.05$ and is used instead of $M = 1$ to avoid potential shock wave issues due to the fact that the flow at the throat is within the transonic range. Static pressure and total temperature $P = 2577$ [kPa] and $T_0 = 3668$ [K] are specified as the two remaining throat parameters.

IX. Calculations

Speed of Sound depends on temperature and can be calculated using the following formula:

$$c=331.5\sqrt{\frac{\theta+273.15}{273.15}}=331.5\sqrt{1+\frac{\theta}{273.15}} \quad \theta \text{ in } ^\circ\text{c}$$

By using above formula

Speed of Sound has been calculated as 1060.95 m/sec. For Mach Number 1.05, Velocity at nozzle throat has been calculated as 1114 m/sec.

X. To Determine The Best Design Option Configuration From (3clover, 4clover And 5 Clover)

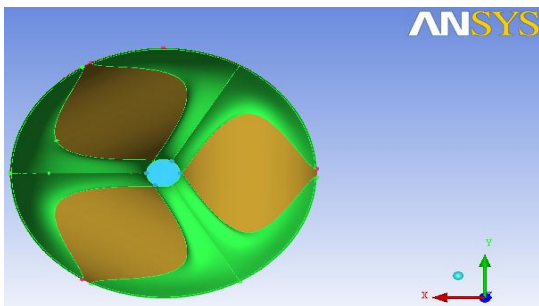


Fig.5 shows rocket nozzle with 3 clovers

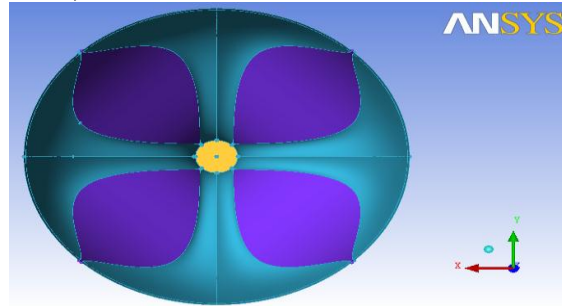


Fig.6 shows rocket nozzle with 4 clovers

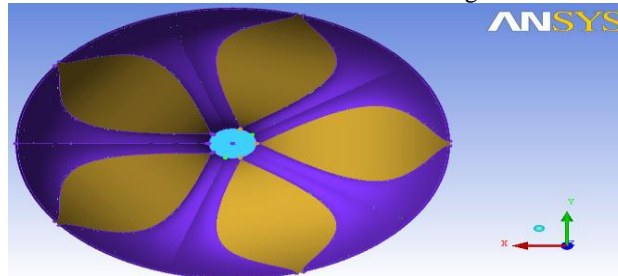


Fig.7 shows rocket nozzle with 5 clovers

XI. The Below Figs Shows 3, 4 And 5 Clovers/Gates Rocket Nozzle After Meshing.

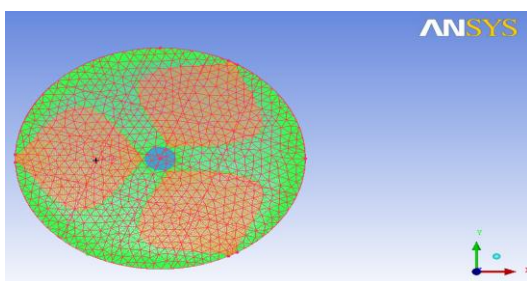


Fig.8 shows rocket nozzle with 3 clovers

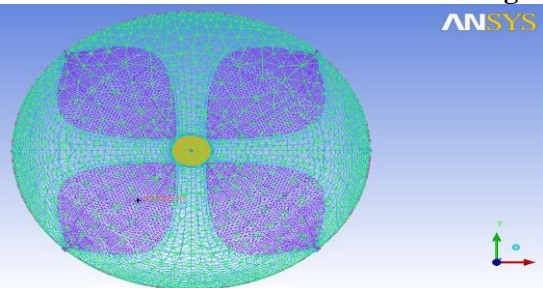


Fig.9 shows rocket nozzle with 4 clovers

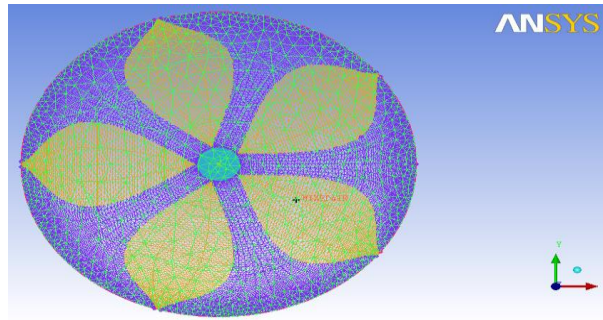


Fig.10 shows rocket nozzle with 5 clovers

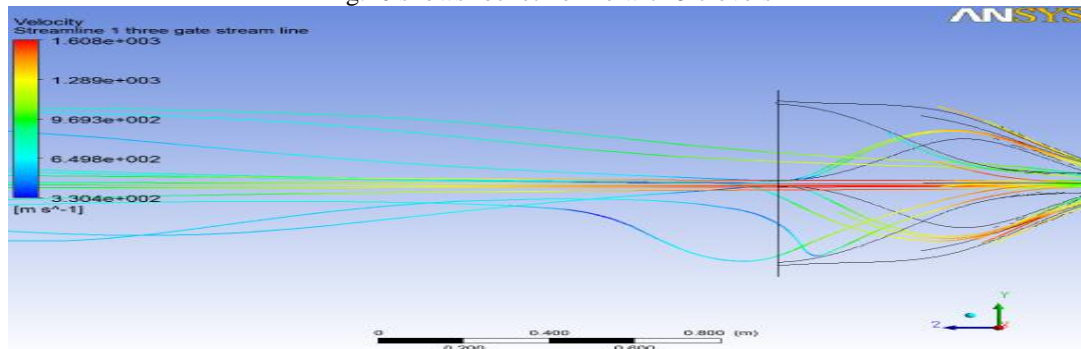


Fig.11 Streamlines for 3 clover nozzle

If you observe the above figures the streamlines across nozzle for 3 clovers are not well streamlined clearly shown in Fig 11. Due to this randomness behavior of streamlines and vortex flows it affects the pressure and velocity distribution across the nozzle.

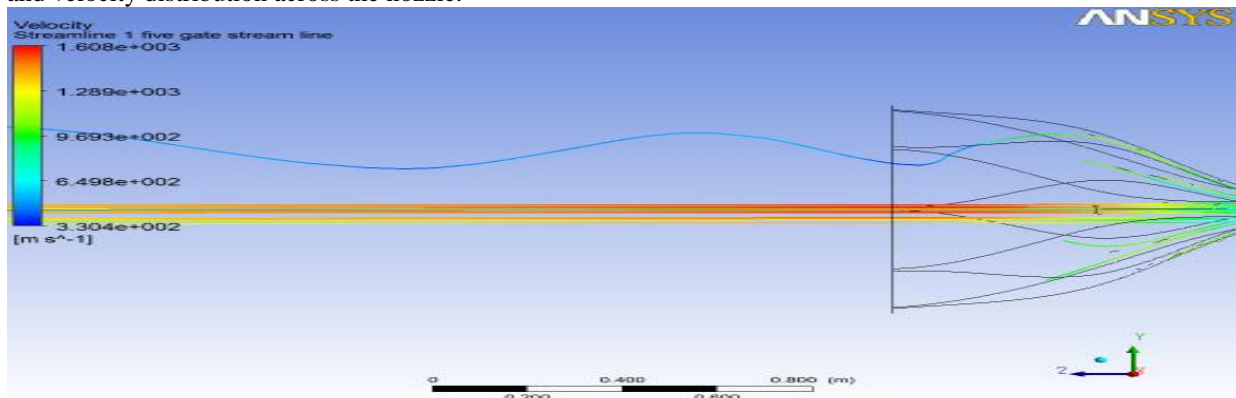


Fig.12 Streamlines for 5 clover nozzle.

If you observe the above figures the streamlines across nozzle for 5 clovers are some that streamlined clearly shown in Fig 12 as compared to 3 clover nozzle.

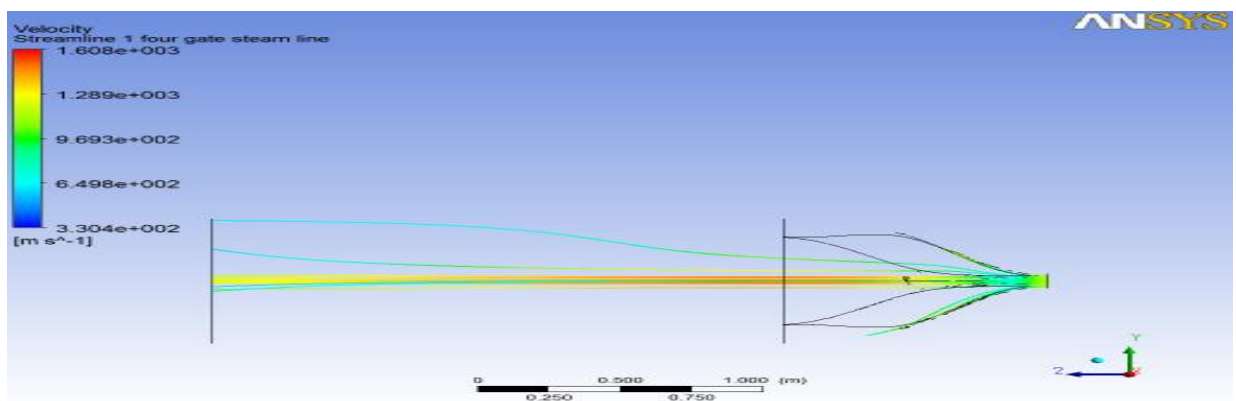


Fig.13 Streamlines for 4 clover nozzle

If you observe the above figures has obtained the effective stream-lined flow compare to other two nozzles (3 gate, 5gate). The velocity distribution and pressure distribution are effective for four clover nozzle when compared to other two nozzles (3 gate, 5gate).

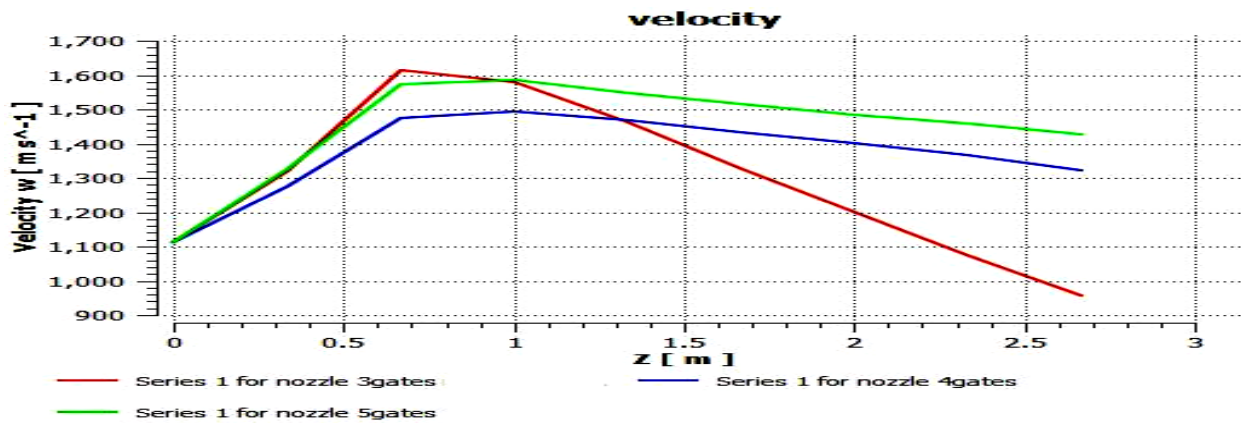


Fig 14 Comparison of velocities of 3, 4 and 5 clover

The above figure shows the comparison of velocities of 3, 4 and 5 clover/gates. From the above figure if you observe the velocities at end of nozzle are as follows.

Clovers/Gates	Velocities(m/s)
3	960
4	1320
5	1420

XII. Mass Flow Rate And Impulse For 3 Clover/Gates

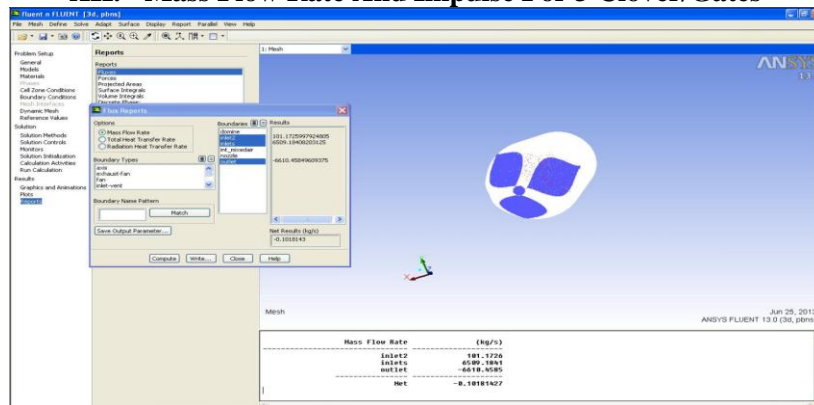


Fig 15 mass flow rate for 3 gates

From the figure if you observe the mass flow rate for 3 gates is 6610kg/s.

And we know from the previous fig the velocity at end of the nozzle for 3 gates is 960 m/s.

$$\text{Impulse (I)} = \text{mass flow rate (m)} * \text{velocity (v)} \Rightarrow I = 6610 * 960 = 6345600 \text{ kg m/s}^2 \Rightarrow I = 6345.6 \text{ kN}$$

XIII. Mass Flow Rate And Impulse For 4 Clover/Gates

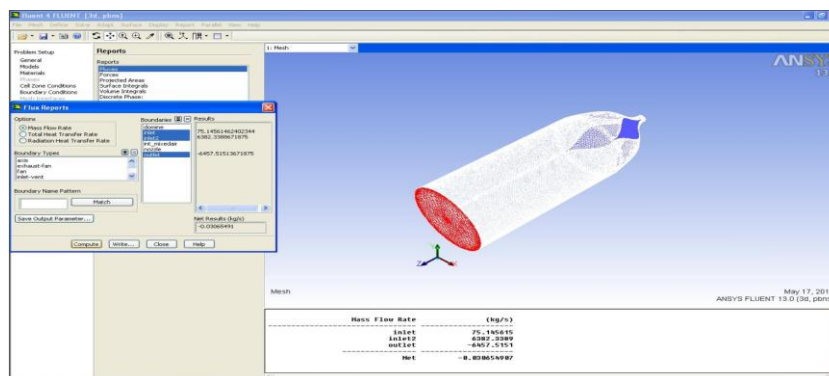


Fig 16 mass flow rate for 4 gates

From the figure if you observe the mass flow rate for 4 gates is 6457kg/s

And we know from the previous fig the velocity at end of the nozzle for 4 gates is 1320 m/s

Impulse (I) =mass flow rate (m)*velocity (v) → I=6457*1320=8523240 kgm/s² → I=8523.2KN

XIV. Mass Flow Rate And Impulse For 5 Clover/Gates

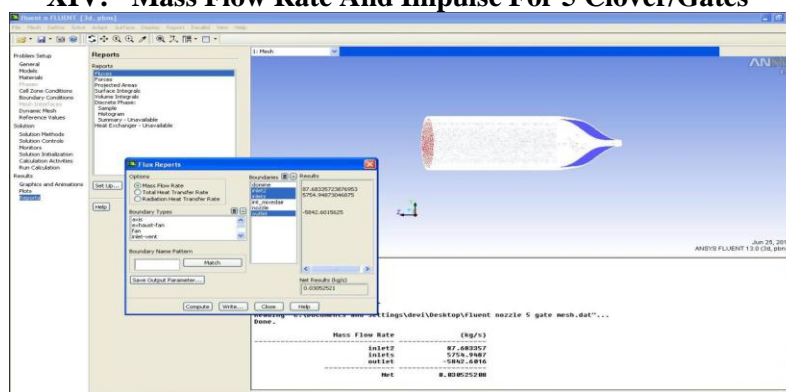


Fig 17 mass flow rate for 5 gates

From the figure if you observe the mass flow rate for 5 gates is 5842kg/s

And we know from the previous fig the velocity at end of the nozzle for 5 gates is 1420 m/s

Impulse (I) =mass flow rate (m)*velocity (v) → I=5842*1420=8295640 kgm/s² → I=8295.6KN

XV. Discussion On Nozzles

1. Nozzle with 3 gates:

In this nozzle, due to larger space of the gates, the mass flow rate and velocity attained by the nozzle are 6610kg/s and 960m/s. The velocity attained by the nozzle is lower than as compared to the other two nozzles, and the Impulse in 3clovers/gates is 6345.6KN is also lower than as compared to the other two nozzles, and the streamlines are not well streamlined. Hence it is not suggested.

2. Nozzle with 4 gates:

In this nozzle, the streamlines across nozzle and pressure distribution and velocity are moderate. This nozzle obtained the effective stream-lined flow compared to other two nozzles. The velocity drop is also moderate. The mass flow rate and velocity attained by the nozzle are 6457kg/s and 1320m/s, and the Impulse in 4clovers/gates is 8523.2KN is greater than as compared to the other two nozzles, Vortex flows are less. It is one of the suggested and effective designs of the nozzle.

3. Nozzle with 5 gates:

In this nozzle, the velocity distribution and pressure distribution are as effective as four gate nozzle. The mass flow rate and velocity attained by the nozzle are 5842kg/s and 1420m/s, and the Impulse in 5clovers/gates is 8295.6KN is lower than 4 clovers/gates. The streamlines are not well streamlined as compared to the 4 gate nozzle.

XVI. Comparison Of Numerical Simulation To A Predefined Mach Number Distribution Of Inviscid And Viscous Simulation.

A. INVISCID SIMULATION

CFD Boundary Conditions

Fluid – Kerosene – Vapor

Chemical Formula – C₁₂H₂₄

Density – 7.1 Kg/m³

Thermal Conductivity -0.0178 w/m-k

For Nozzle Throat

Velocity = 1114 m/sec

Supersonic Gauge Pressure = 2475.6 K Pa (2577 Kpa – Operating Pressure (101325 Pa))

Temperature = 3668 K

For Air Intake = Pressure Inlet

For Nozzle Outlet = Pressure Outlet

Operating Pressure = 101325 Pa

Wall Temperature = 500 K

1. PRESSURE DISTRIBUTION

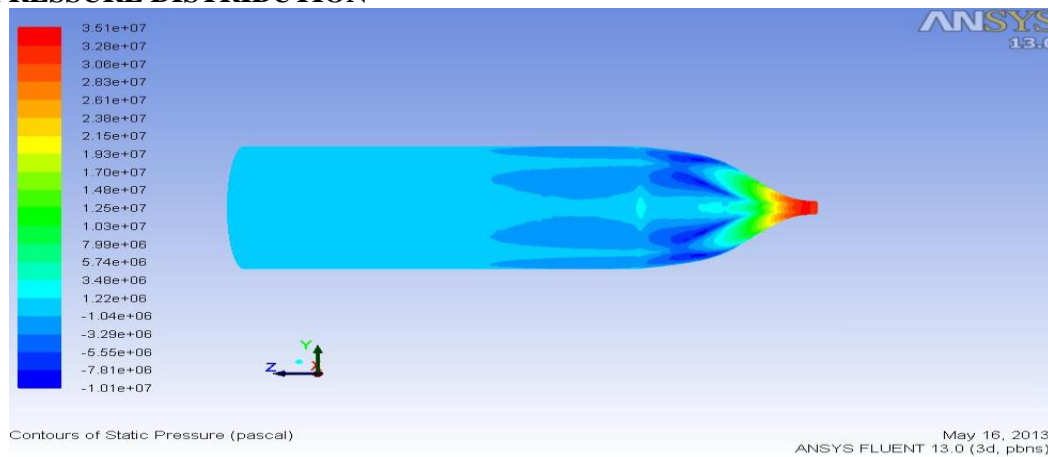


Fig 18 pressure distribution

The above figure shows how the distribution of pressure takes place through the nozzle. If you observe pressure is maximum near the throat and it has reached nearly 3.51×10^{07} pa and afterword's the pressure starts reducing at the end of the nozzle, it has reached a value 0.18×10^{07} pa. This reduction in pressure is converted into velocity

2. VELOCITY DISTRIBUTION

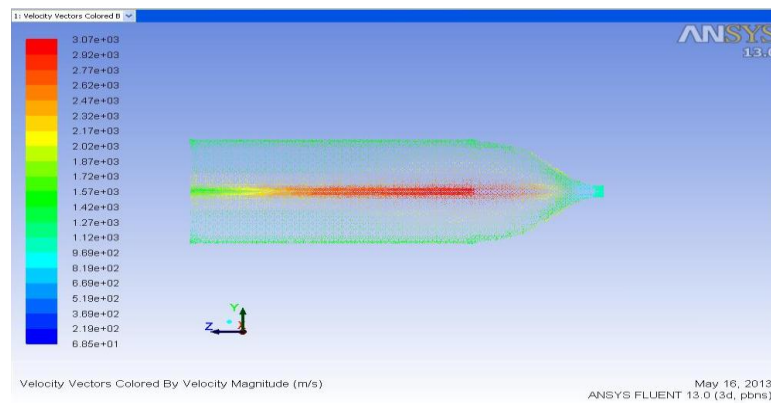


Fig 19 velocity distribution

The above figure shows how the distribution of velocity takes place through the nozzle. If you observe velocity is maximum near the centre line and it has reached nearly 3.07×10^{03} m/s and at the end of the nozzle it has reached a value 2.9×10^{01} m/s.

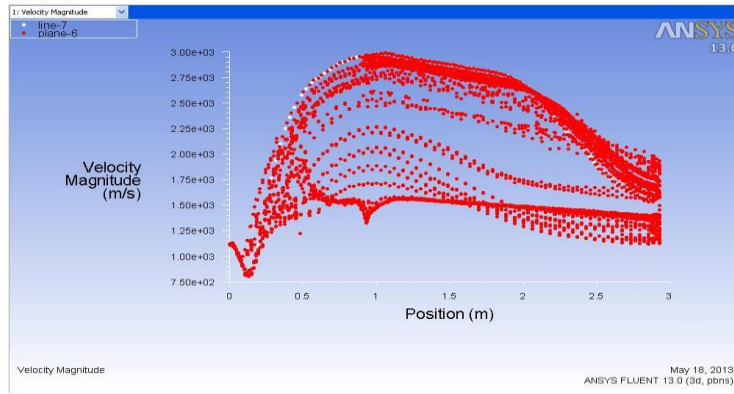


Fig 20 velocity distribution through the centre plane.

The above figure shows how the distribution of velocity takes place through the nozzle. If you observe white dots shows velocity distribution through the centre line. And the red dots show velocity distribution through the centre plane YZ.

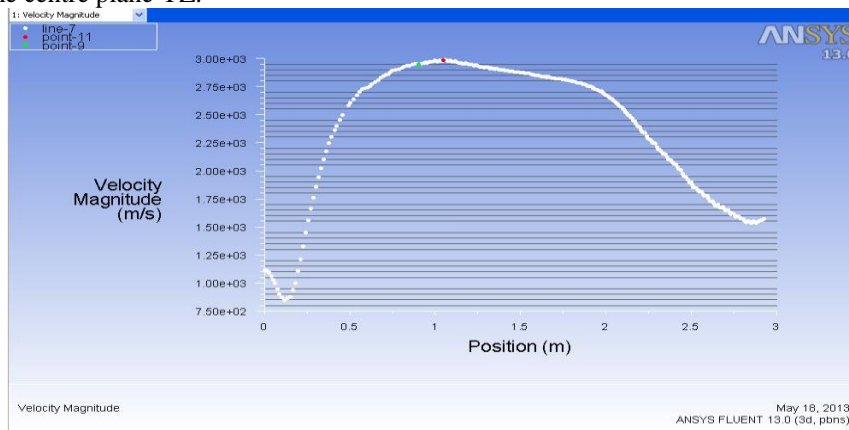


Fig 21 velocity distribution through the centre line.

The above figure shows how the distribution of velocity takes place through the nozzle. If you observe velocity is maximum near the centre line at a distance 1.05 m it has reached nearly 3.07×10^3 m/s and at the end of the nozzle that is at distance 0.9 m it has reached a value 2.99×10^3 m/s.

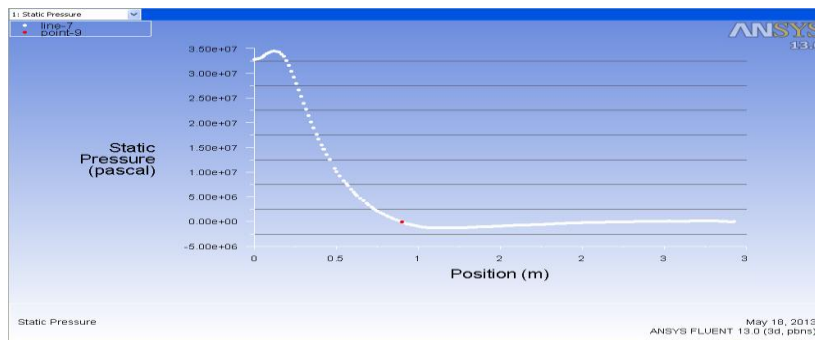


Fig 22 pressure distribution through the centre line.

The above figure shows how the distribution of pressure takes place through the nozzle. If you observe pressure is maximum near the throat once upon a time it has reached nearly 3.51×10^7 pa at a distance from throat 0.12 m and afterword's the pressure starts reducing at the end of the nozzle that is at a distance 0.9 m from throat it has reached a value 0.18×10^7 pa. This reduction in pressure is converted into velocity.

3. INVISCID FLOW RESULTS:

The inviscid CFD area averaged $M_{(z)}$ and $P_{(z)}$ results to the predefined $M_{(z)}$ distribution and the isentropic pressure calculated using the $M_{(z)}$ distribution respectively. Computational results predict outlet

values of $M_e=2.69$ and pressure $P_e=183.1\text{Kpa}$. In comparison, the predefined $M(z)$ gives $M_e=2.75$ and $P_e=170.0\text{Kpa}$ and translate into differences of 2.1% and 7.6% respectively.

B. VISCOUS SIMULATION

CFD Boundary Conditions

Fluid – Kerosene – Vapor

Chemical Formula – $\text{C}_{12}\text{H}_{24}$

Density – 7.1 Kg/m^3

Thermal Conductivity -0.0178 w/m-k

Viscosity – $7\text{ e-}08\text{ Kg/m-s}$

For Nozzle Throat

Velocity = 1114 m/sec

Supersonic Gauge Pressure = 2475.6 K Pa (2577 Kpa – Operating Pressure (101325 Pa))

Temperature = 3668 K

For Air Intake = Pressure Inlet

For Nozzle Outlet = Pressure Outlet

Operating Pressure = 101325 Pa

Wall Temperature = 500 K

K- ξ Turbulence has been used with 5% as turbulence intensity at boundaries.

1. PRESSURE DISTRIBUTION

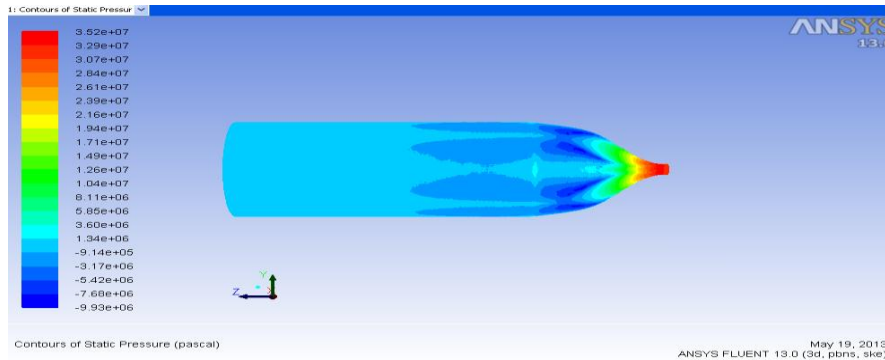


Fig 23 pressure distribution

The above figure shows how the distribution of pressure takes place through the nozzle. If you observe pressure is maximum near the throat and it has reached nearly 3.52×10^{07} pa and afterword's the pressure starts reducing at the end of the nozzle it has reached a value 2.47×10^{06} pa. This reduction in pressure is converted into velocity.

2. VELOCITY DISTRIBUTION

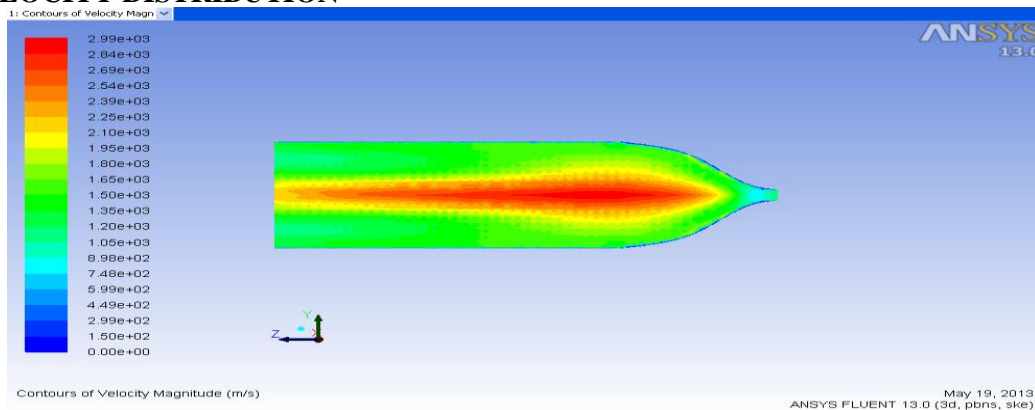


Fig 24 velocity distribution

The above figure shows how the distribution of velocity takes place through the nozzle. If you observe velocity is maximum near the centre line and it has reached nearly 2.99×10^{03} m/s and at the end of the nozzle it has reached a value 2.95×10^{03} m/s.

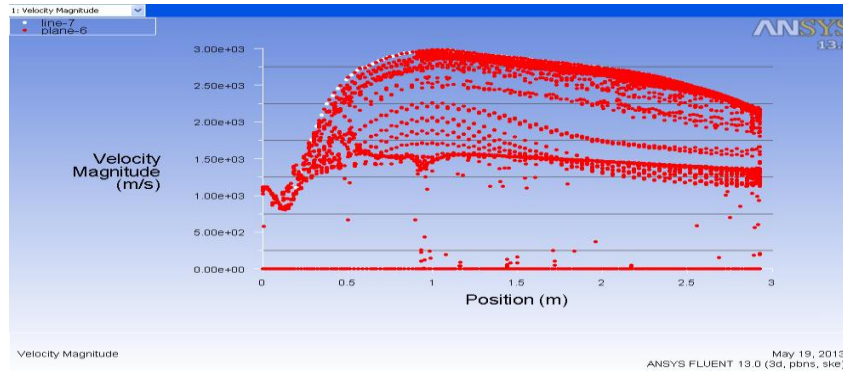


Fig 25 velocity distribution through the centre plane.

The above figure shows how the distribution of velocity takes place through the nozzle. If you observe white dots shows velocity distribution through the centre line. And the red dots show velocity distribution through the centre plane YZ.

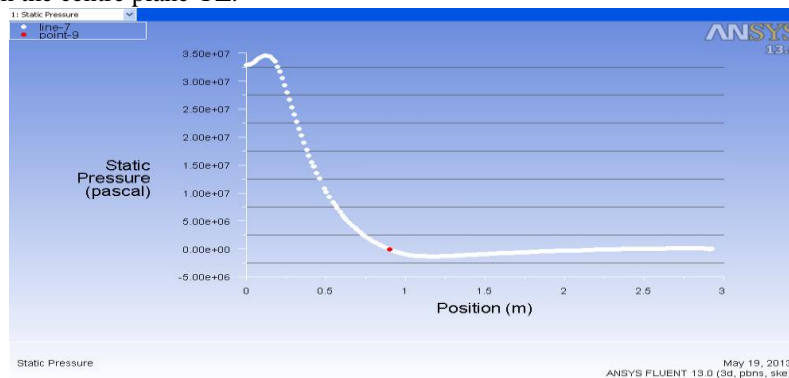


Fig 26 pressure distribution through the centre line.

The above figure shows the distribution of pressure along the nozzle. If you observe pressure is maximum near the throat and it has reached nearly 3.50×10^7 pa at a distance from throat 0.12 m and afterword's the pressure starts reducing this reduction in pressure is converted into velocity.

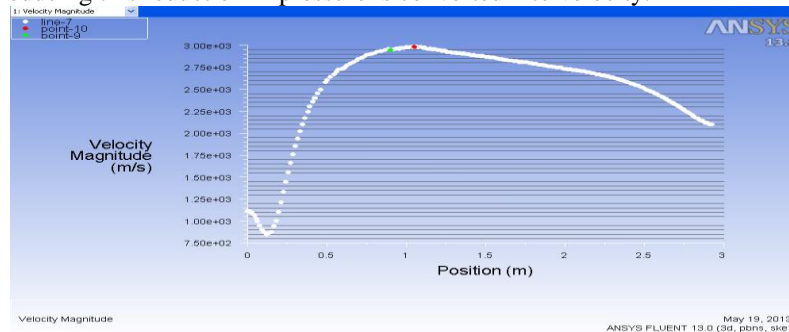


Fig.27 velocity distribution through the centre line.

The above figure shows how the distribution of velocity takes place through the nozzle. If you observe velocity is maximum near the centre line at a distance 1.05 m it has reached nearly 3.00×10^3 m/s and at the end of the nozzle that is at distance 0.9m it has reached a value 2.95×10^3 m/s.

3. INVISCID FLOW RESULTS:

The inviscid CFD area averaged $M_{(z)}$ and $P_{(z)}$ results to the predefined $M_{(z)}$ distribution and the isentropic pressure calculated using the $M_{(z)}$ distribution respectively. Computational results predict outlet values of $M_e=2.64$ and pressure $P_e= 247$ Kpa. In comparison, the predefined $M_{(z)}$ gives $M_e=2.75$ and $P_e=170.0$ Kpa and translate into differences of 4% and 31.1% respectively.

XVII. Conclusion

- Based on the provided geometry and fluid property inputs, the present theory is capable of generating three-dimensional diverging sections of a converging-diverging rocket nozzle.

- Based on the flow analysis and impulse it is found that nozzle with 4 clovers/gates provides better results when compared with the other i.e., 3 or 5 clovers/gates and it is one of the suggested and effective design of the nozzle.
- Results are provided for one configuration only, which is unlikely to be an optimum configuration and is not representative of all configurations
- Inviscid area-averaged computational results are within 2.1% of the predefined outlet Mach number of 2.75 and 7.6% of the isentropic pressure predicted at the outlet.
- Viscous computational results obtained using the k-e turbulence model under-predict the predefined outlet Mach number by 4% which is acceptable.
- Observations from the total pressure field show that the flow does not become fully developed and that viscous effects are contained within the boundary layers at each wall. Since the flow is not isentropic within the boundary layer, there is corresponding pressure losses due to the increase in friction and thus a 34.9% pressure variation at the outlet is observed when compared to the inviscid analysis.

References

- [1]. Turner, M. J. L., *Rocket and Spacecraft Propulsion: Second Edition*, Praxis Publishing Ltd., 2005.
- [2]. Tajmar, M., *Advanced Space Propulsion Systems*, Springer-Verlag/Wien, 2003.
- [3]. Sutton, G. P., *History of Liquid Propellant Rocket Engines*, American Institute of Aeronautics and Astronautics, 2006.
- [4]. Daines, R. and Segal, C., "Combined Rocket and Air breathing Propulsion Systems for Space- Launch Applications," *Journal of Propulsion and Power*, Vol. 14, No. 5, 1998, pp. 605–12.
- [5]. White, F. M., *Fluid Mechanics*, Boston: McGraw-Hill, 5th ed., 2003.
- [6]. Ejector air intake design method for a novel rocket-based combined-cycle rocket nozzle by Timothy S. Waung, Carleton University Ottawa, Ontario, Canada April 2010
- [7]. Manski, D. and Hagemann, G., "Influence of Rocket Design Parameters on Engine Nozzle Efficiencies," *Journal of Propulsion and Power*, Vol. 12, No. 1, 1996, pp. 41–7.
- [8]. Korst, H. H., Addy, A. L., and Chow, W. L., "Installed Performance of Air-Augmented Nozzles Based on Analytical Determination of Internal Ejector Characteristics," *Journal of Aircraft*, Vol. 3, No. 6, November–December 1966, pp. 498–506.
- [9]. Nayem Jahingir, M. and Huque, Z., "Design Optimization of Rocket-Based Combined-Cycle Inlet/Ejector System," *Journal of Propulsion and Power*, Vol. 21, No. 4, July–August 2005, pp. 650–5.
- [10]. Etele, J., *Computational Study of Variable Area Ejector Rocket Flow fields*, Ph.D. thesis, University of Toronto, Institute for Aerospace Studies, Toronto, 2004.
- [11]. Etele, J., Sislian, J. P., and Parent, B., "Effect of Rocket Exhaust Configurations on Ejector Performance in RBCC Engines," *Journal of Propulsion and Power*, Vol. 21, No. 4, July– August 2005, pp. 656–66.
- [12]. White, F. M., *Viscous Fluid Flow*, Boston: McGraw-Hill, 3rd ed., 2006.
- [13]. ANSYS, Inc., *ANSYS CFX, Release 11.0 User Guide*, 2006.